

See discussions, stats, and author profiles for this publication at: <https://www.researchgate.net/publication/44627985>

# Kinetic processes in supercooled monosaccharides upon melting: Application of dielectric spectroscopy in the mutarotation studies of D-ribose

ARTICLE in THE JOURNAL OF CHEMICAL PHYSICS · MAY 2010

Impact Factor: 2.95 · DOI: 10.1063/1.3408286 · Source: PubMed

---

CITATIONS

14

---

READS

31

## 7 AUTHORS, INCLUDING:



[Patryk Włodarczyk](#)

Institute of Non-Ferrous Metals

51 PUBLICATIONS 563 CITATIONS

SEE PROFILE



[Kamil Kaminski](#)

University of Silesia in Katowice

86 PUBLICATIONS 975 CITATIONS

SEE PROFILE



[Mateusz Dulski](#)

University of Silesia in Katowice

37 PUBLICATIONS 211 CITATIONS

SEE PROFILE



[Jerzy Ziolo](#)

instytut fizyki

78 PUBLICATIONS 1,323 CITATIONS

SEE PROFILE

# Kinetic processes in supercooled monosaccharides upon melting: Application of dielectric spectroscopy in the mutarotation studies of D-ribose

P. Włodarczyk,<sup>1,a)</sup> K. Kaminski,<sup>1</sup> S. Haracz,<sup>1</sup> M. Dulski,<sup>1</sup> M. Paluch,<sup>1</sup> J. Ziolo,<sup>1</sup> and M. Wygledowska-Kania<sup>2</sup>

<sup>1</sup>*Institute of Physics, Silesian University, Uniwersytecka Street 4, 40-007 Katowice, Poland*

<sup>2</sup>*Department of Dermatology, Silesian Medical University in Katowice, Francuska Street 20/24, 40-027 Katowice, Poland*

(Received 15 December 2009; accepted 3 April 2010; published online 20 May 2010)

Dielectric spectroscopy has been recently used to monitor mutarotation in undercooled D-fructose. This method can be viewed as a universal method to study mutarotation phenomenon in the whole family of monosaccharides. In this paper, we studied kinetics of mutarotation of anhydrous D-ribose at ambient pressure as well as pressure effect on the rate constant of this process. Ribose mutarotation behavior is compared to the one obtained for D-fructose. In addition, we attempted to determine the “direction” of mutarotation in undercooled monosaccharides after quenching the melted sample. To this end, analysis of dipole moments of different tautomers of D-fructose and D-ribose have been performed. Conformational analysis of studied carbohydrates was done with use of density functional theory. Geometry optimizations as well as calculations of dipole moments were done on the 6-311++G(d,p)/B3LYP level. Finally, it turned out that data obtained from the mutarotation experiment might be helpful in understanding the origin of  $\gamma$ -process occurring in the whole family of carbohydrates. © 2010 American Institute of Physics. [doi:10.1063/1.3408286]

## I. INTRODUCTION

Carbohydrates are biological compounds, which are essential for life processes. Therefore, many studies devoted to them have been performed and published in large number of papers.<sup>1–10</sup> Chemically, carbohydrates are polihydroxy ketones (ketoses) or aldehydes (aldoses), which tend to form hemiacetal rings. Chain structure is unstable and cyclic form is always dominant. Monosugar ring can acquire pyranose (six-membered), furanose (five-membered), septanose (seven-membered), or oxetanose (four-membered) form. In most cases, monosaccharide samples exist as a pure pyranoses or pyranose-furanose mixtures. This depends on state of matter and the kind of monosaccharide. Significant amount of furanoses can be found in pentoses (e.g., ribose, arabinose, xylose, etc.) or ketohexoses (e.g., fructose, psicose, sorbose, etc.)<sup>11,12</sup> in the liquid state, whereas septanose or oxetanose rings are rather exotic. During the cyclization of the chain carbohydrate, the new chirality center is formed, usually on first or second carbon atom. Therefore, these two forms of certain carbohydrate are called anomers and they need to be distinguished. As hydroxyl group attached to this chiral carbon is oriented up in the Haworth projection,<sup>12</sup> the sugar is named  $\beta$ -anomer. Opposite orientation is attributed to  $\alpha$ -anomer. Carbohydrates' crystals are usually formed by the pure  $\alpha$  or  $\beta$  pyranose forms. Contrary to the crystalline state, all tautomeric forms can coexist together in the equilibrium liquid state. Therefore, when one melts or dissolves crystalline sample, process of equilibration in saccharide

sample is initialized and this phenomenon is known as mutarotation. To be more precise, mutarotation term is given to the change of specific optical rotation during these conversions. Rings are being rebuilt from pyranoses to different anomers or different rings (to furanoses). Despite of the fact that mutarotation was discovered more than 100 years ago, there are still many aspects of this process that need to be clarified. Therefore, several papers about this process have been recently published.<sup>13–18</sup> They concern mainly mutarotation in supercooled liquid and glassy state.

There are few experimental techniques employed for studying mutarotation, i.e., polarimetry, Raman spectroscopy, IR spectroscopy, chromatography, and recently also dielectric spectroscopy.<sup>13</sup> The first method is very popular and it is the best choice for studying this phenomenon in diluted solutions. For study of pure or highly concentrated sugars, other methods are preferable. Dielectric spectroscopy can be used to monitor this process in supercooled liquid state, where structural relaxation can be observed, whereas in the glassy state the best choice would be Raman or IR spectroscopy.

In this paper, for the first time, we present studies on mutarotation's kinetics of anhydrous D-ribose in the supercooled liquid state at different thermodynamic conditions. We have chosen D-ribose for analysis, because it is biologically important monosaccharide. D-ribose is a part of biologically important molecules, especially ribonucleic acid, RNA, and energy storing molecule, adenosine triphosphate (ATP). Therefore this saccharide is present in almost every cell of living organisms, from viruses to mammals. D-ribose is used as a dietary supplement to decrease muscle fatigue.

<sup>a)</sup>Electronic mail: pwlodarc@us.edu.pl.

Oral intake of this monosaccharide boosts ATP recovering in the muscles. Thus it is recommended for people suffering from fibromyalgia and poor cardiovascular health.

As we are interested in examination of mutarotation's behavior in supercooled liquid state of D-ribose, we have used dielectric spectroscopy as a experimental technique to monitor this process. Broadband dielectric spectroscopy (BDS) is powerful tool to investigate molecular dynamics of glass forming liquids. One can observe relaxation processes in liquid and glassy state connected with dipoles' reorientation. Structural relaxation ( $\alpha$ -process) is the slowest observed process and it governs glass transition. Faster processes (secondary modes) are generally related to more restricted in space local movements of molecules. Description of mutarotation kinetics can be performed by monitoring changes of structural relaxation process in time. The characteristic structural relaxation time ( $\tau_\alpha$ ) as well as static permittivity ( $\epsilon_s$ ) are the key parameters in the further analysis of the kinetics. Kinetics curves are constructed by plotting these parameters versus time. In the next step, data are fitted to the exponential first order equation and rate constant is obtained.

One of the main goals of this paper is determination of mutarotation direction upon quenching the melted sample. Variation of static permittivity observed during mutarotation in quenched sample are correlated with the changes of average dipole moment value. Every tautomer has different characteristic value of dipole moment, and the ratio of tautomers is changing during transformations. If one knows behavior of static permittivity of sample and dipole moment of every tautomer, it would be possible to make prediction of mutarotation's direction. Static permittivity can be obtained easily from dielectric measurements, while dipole moments can be calculated by different methods. In this work, dipole moments were calculated by means of density functional theory, one of the most popular quantum mechanics (QM) method. Calculations of dipole moments were preceded by geometry optimizations of every tautomer.

Studies of mutarotation's influence on the behavior of the local secondary mode ( $\gamma$ -process) is the final aim of this paper. The origin of fast  $\gamma$ -process observed in vicinity of glass transition is still unresolved issue. We have performed measurements of local dynamics before and after entire sample equilibration, and we have found that some of features of this relaxation are influenced by mutarotation. Consequently, observed changes of  $\gamma$ -process turn out to be helpful in explaining its molecular nature.

## II. EXPERIMENTAL AND COMPUTATIONAL

Anhydrous D-ribose of 99% purity was purchased from Merck. Dielectric measurements were performed just after quick melting of the sample. One should note that caramelization (decomposition) usually occurs during the sample melting. However, melting point of D-ribose is equal to 368 K (95 °C) and the melting time was less than 1 min. In such conditions, i.e., quick melting at relatively low temperature, the possibility of caramelization of D-ribose can be ruled out. Melted sample was quenched to the room temperature

with use of metal plate (high cooling rate). Thereafter, sample was heated in the Alpha dielectric spectrometer with gradient 5 K/min to the temperature of measurement. Isothermal measurements were performed at five different temperatures in the range 293 to 305 K with 3 K step. These measurements were carried out using a Novo-Control GMBH Alpha dielectric spectrometer ( $10^2$ – $10^7$  Hz). The temperature was controlled by the Quattro Cryosystem by Novo-Control, with use of nitrogen-gas cryostat. Temperature stability of the sample was better than 0.1 K.

In the case of pressure measurements, capacitor filled with the test material was placed in high pressure chamber and compressed using of silicone fluid via a piston in contact with a hydraulic press. The sample capacitor was sealed and mounted inside Teflon membranes to separate it from the silicon oil. Pressure was measured by a Nova Swiss tensometric meter with resolution of 0.1 MPa. The temperature was controlled within 0.1 K by means of liquid flow from a thermostatic bath.

Computations were carried out by the noncommercial ORCA quantum package.<sup>19</sup> Program provides efficient optimizations algorithms. Computations were done mainly for D-ribose, but also for D-fructose. We have compared these two monosaccharides to avoid coincidental compatibility between dipole moments and static permittivity change. This will be explained in great detail later in this paper. The first task was finding most stable conformers of every tautomeric form. In case of pyranoses, most stable forms can be easily predicted, without of lot of computations. The chair structure with the largest number of hydroxyl groups in equatorial positions is preferable due to the unfavorable diaxial interactions in case of hydroxyl groups in axial positions. The only exception is hydroxyl group attached to the anomeric carbon, where so called exoanomeric effect could be deciding. Four pyranosidic tautomers, i.e.,  $\alpha$ -D-fructopyranose,  $\beta$ -D-fructopyranose,  $\alpha$ -D-ribopyranose, and  $\beta$ -D-ribopyranose were modeled by hand and then optimized on the B3LYP/6-311++G(d,p) level. For every tautomer, several conformations were tested. They had different orientation of hydroxyl groups (clockwise or counterclockwise) and in the case of D-fructose also different orientation of hydroxymethyl group (different rotamers). D-ribose has only five carbon atoms and it does not have hydroxymethyl group ( $-\text{CH}_2\text{OH}$ ) in pyranose form, thus there are no different rotamers of D-ribopyranose. Optimizing furanoses is more complicated. For every furanosidic form, we have found approximately 25 conformers from randomly generated structures. Geometry of every furanosidic form was also optimized on the B3LYP/6-311++G(d,p) level. We have found lot of conformers with energy differences approximately few kJ/mol from the lowest energy form. This is quite inconvenient situation because those forms have almost the same energy while their dipole moments are often significantly different. To resolve this problem, we calculated averaged dipole moments from five most stable conformers for every furanose. We have compared energies of five more stable conformers. We have obtained distribution of those five energetic states by means of Boltzmann relations

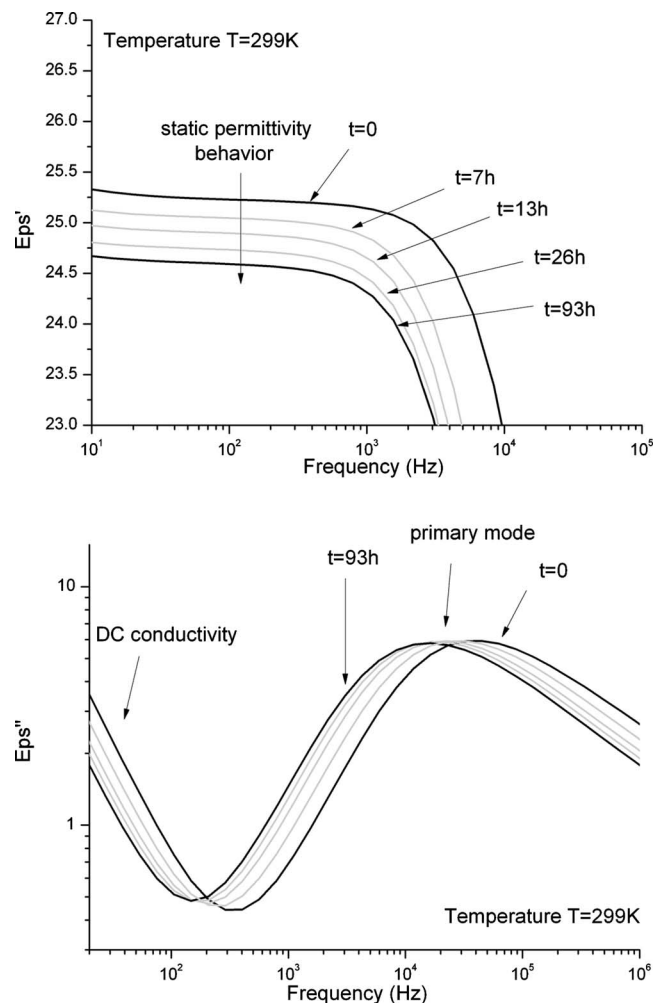


FIG. 1. Evolution in time of dielectric spectra.

(distribution ratio of two states  $n_i$  to  $n_j$  is given by the equation  $n_i/n_j = \exp(-\Delta E/kT)$ ). Dipole moment was obtained as weighted average where calculated distributions were treated as a weight.

### III. RESULTS AND DISCUSSION

We have measured anhydrous D-ribose by means of dielectric spectroscopy at ambient pressure in the narrow temperature range, i.e., from 293 to 305 K, with 3 K step. Moreover we have performed measurement at elevated pressure, equaled to 400 MPa at 299 K. By monitoring changes of structural relaxation process with time at established thermodynamic conditions we have obtained kinetics curves. They were prepared by plotting structural relaxation time ( $\tau_\alpha$ ) and static permittivity ( $\epsilon_s$ ) versus time. In Fig. 1 we have shown evolution in time of dielectric spectra. Structural relaxation curve is shifting towards lower frequencies. As one can see, relaxation time increases in time, while static permittivity slightly drops down. We have found that obtained data can be satisfactory described by first order kinetic equation

$$\tau_\alpha = \exp(-k_{\tau_\alpha} \cdot t) + C_1, \quad (1)$$

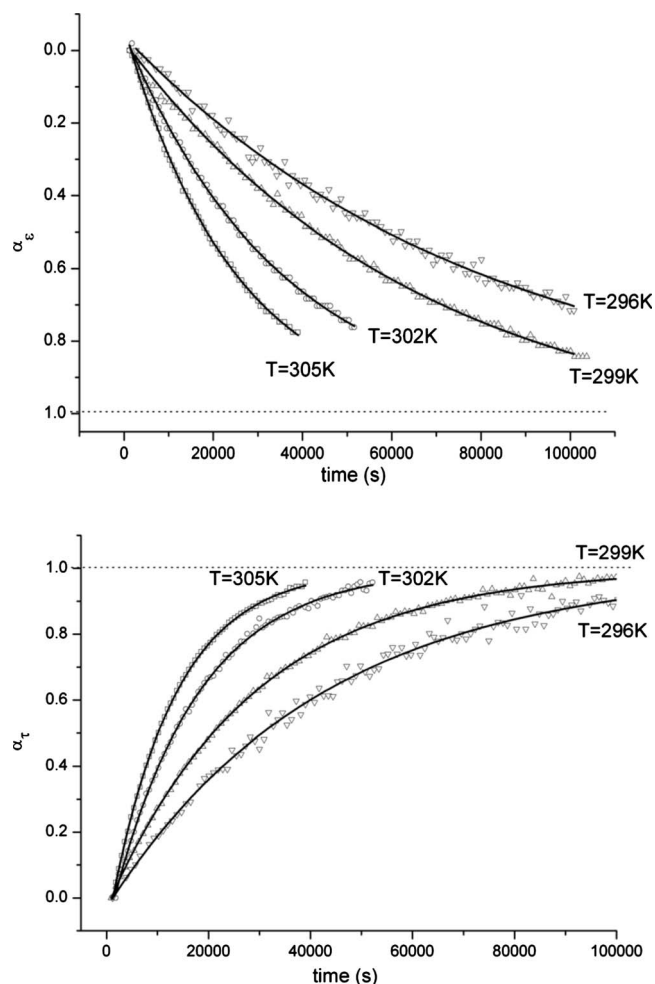


FIG. 2. Kinetic curves obtained by analysis of static permittivity (upper panel) and relaxation time (bottom panel) time dependence.

$$\epsilon_s = \exp(-k_{\epsilon_s} \cdot t) + C_2, \quad (2)$$

where  $k_{\epsilon_s}$  and  $k_{\tau_\alpha}$  are corresponding values of rate constants and  $t$  is time. Rate constant is the key parameter which describes kinetics. With use of rate constant  $k$ , reaction half-time ( $\tau_{1/2}$ ) can be calculated from the equation

$$\tau_{1/2} = \frac{\ln(2)}{k}. \quad (3)$$

Above relation is valid only for first order kinetics. In Fig. 2 we have compared kinetic curves for different temperatures on one diagram. To this end, we have substituted parameters  $\tau_\alpha$  and  $\epsilon_s$  by degree of reaction  $\alpha$  in the manner described below,

$$\alpha_\tau = \frac{\tau_\alpha - \tau_{\alpha_p}}{\tau_{\alpha_k} - \tau_{\alpha_p}}, \quad (4)$$

$$\alpha_\epsilon = \frac{\epsilon_s - \epsilon_{s_p}}{\epsilon_{s_k} - \epsilon_{s_p}}. \quad (5)$$

By use of dimensionless degree of reaction  $\alpha$  instead of original parameters, kinetic curves are no shifted vertically on one diagram. Degree of reaction can vary from 0 to 1,



TABLE I. Kinetic parameters for D-ribose.

T (K)	$k_{\tau_{\alpha}}$ ( $s^{-1}$ )	$k_{\epsilon_s}$ ( $s^{-1}$ )
296	$2.37 \times 10^{-5}$	$1.17 \times 10^{-5}$
299	$3.48 \times 10^{-5}$	$1.53 \times 10^{-5}$
302	$5.90 \times 10^{-5}$	$2.89 \times 10^{-5}$
305	$7.83 \times 10^{-5}$	$4.03 \times 10^{-5}$

where 0 denotes beginning and 1 denotes end of reaction. In Table I one can find comparison of rate constants  $k_{\tau_{\alpha}}$  and  $k_{\epsilon_s}$ . It turned out that process observed by changes of static permittivity is much slower than the process observed by the changes of structural relaxation time. These differences in time scale are due to the complex character of mutarotation. Mutarotation can be divided into three subprocesses, i.e., pyranose-pyranose and two types of pyranose-furanose transformations. All of them occur at the same time. Behrends *et al.*<sup>18</sup> have noticed that kinetics derived from the analysis of relaxation times changes measured by ultrasonic spectroscopy, represents single subprocess, i.e., only one pathway. Monitoring other parameters by different methods leads to the whole mutarotation description, i.e., average effect. By use of BDS, we have monitored two types of parameters. We assumed that changes of static permittivity describe mutarotation in general, whereas changes of structural relaxation characteristic time provide information about only one transformation pathway, most probably furanose-pyranose conversion. Static permittivity is related to the average value of dipole moment, while structural relaxation time is related to the viscosity of the sample. Anomeric transformation has lower impact on viscosity change than ring conversion. We have found, that in D-glucose which is built of pyranosidic rings only (there is a mixture of  $\alpha$  and  $\beta$ -pyranose in liquid sample), structural relaxation time does not change at all. This experimental fact supports our assumption. Kinetic curves obtained by structural time analysis could be connected with the pyranose-furanose transformation.

Mutarotation has been also studied at elevated pressure in Ref. 20. Sander in cited article has shown that in solutions of D-glucose, pressure exerted on the system (up to 7 MPa) is positively related to the rate of mutarotation. In the other words, pressure speeds up mutarotation. Experiment has been repeated by Andersen *et al.*<sup>21</sup> with much higher pressure exerted on the sample (up to 100 MPa) and the outcome of the experiment was the same. Pressure is connected at isothermal conditions with rate constant ( $k$ ) by the equation<sup>21</sup>

$$\frac{\partial \ln k}{\partial p} = -\Delta V \cdot (RT)^{-1}, \quad (6)$$

where  $R$  is gas constant,  $T$  is the absolute temperature,  $p$  is the pressure, and  $\Delta V$  is activation volume. Pressure can speed up or slow down every reaction. It depends on the sign of activation volume. Transition state, i.e., activated state can have lower ( $\Delta V < 0$ ) or higher molecular volume ( $\Delta V > 0$ ) than the stable structure, i.e., nonactivated state. Sander has assumed that transition state created during mutarotation has rodlike shape and can be easily packed in the space earlier occupied by the ringlike minimum state. Molecular volume

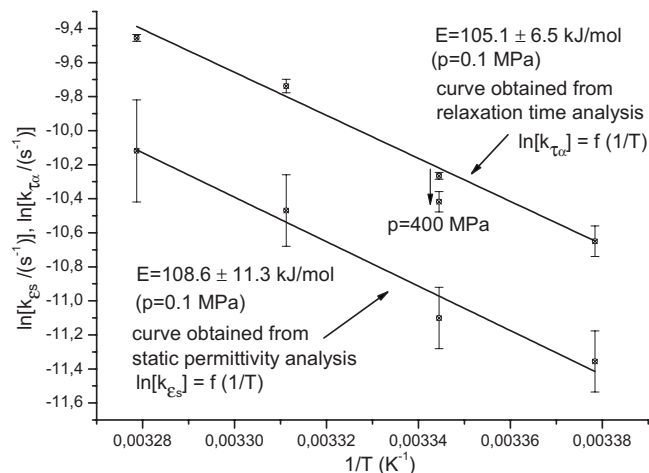


FIG. 3. Temperature dependences of rate constants ( $k_{\tau_{\alpha}}$ ,  $k_{\epsilon_s}$ ) logarithms. Activation energy equaled to 105 kJ/mol was obtained from relaxation time analysis, while energy equaled to 109 kJ/mol was obtained from static permittivity analysis. The point at elevated pressure ( $p=400$  MPa) was obtained also from relaxation times analysis.

of activated state is lower than the molecular volume of non-activated state, thus  $\Delta V < 0$ . Contrary to the refereed studies in D-glucose solutions, we have found that in anhydrous D-ribose pressure exerts opposite effect, although we were able to determine kinetics only by monitoring structural relaxation time. At  $p=400$  MPa and  $T=299$  K, mutarotation was slower than at ambient pressure. The rate constant has changed from  $3.48 \times 10^{-5}$  to  $2.99 \times 10^{-5} s^{-1}$ .

In Fig. 3 we have presented temperature dependences of rate constants logarithms. Arrhenius fits were performed to describe data

$$\ln(k) = C + \Delta E \cdot (RT)^{-1}, \quad (7)$$

where  $\Delta E$  is activation energy,  $T$  is absolute temperature,  $R$  denotes gas constant, and  $C$  is pre-exponential factor which is equivalent to the term describing activation entropy in Eyring equation. Energy of activation of this process is equaled to about 100 kJ/mol (see Fig. 3 for details). The energy is comparable to the one obtained for anhydrous D-fructose.

To understand the nature of mutarotation in supercooled liquid state, one has to know direction of mutarotation upon quenching melted sugar. At melting point temperature, process is extremely fast, which can be predicted by extrapolating temperature dependence of rate constant. We can assume that when crystalline sample is being melted, tautomeric equilibrium (high-temperature equilibrium) is formed within seconds. Complexity of equilibrium forming during the melting process is presented in Fig. 4. In the diagram presented in Fig. 5 two pathways are presented after the melting. Quickly quenched sample becomes glass at temperature  $T=256$  K, but in the case when sample is quenched to the room temperature and equilibrated, glass transition is shifted to the temperature  $T=262$  K. Carbohydrates do not have strictly defined glass transition temperature, because it depends on different tautomers population ratio. For D-ribose, difference in glass transition temperature is about 6 K (see Fig. 6) Furanoses and pyranoses have different glass transition tempera-

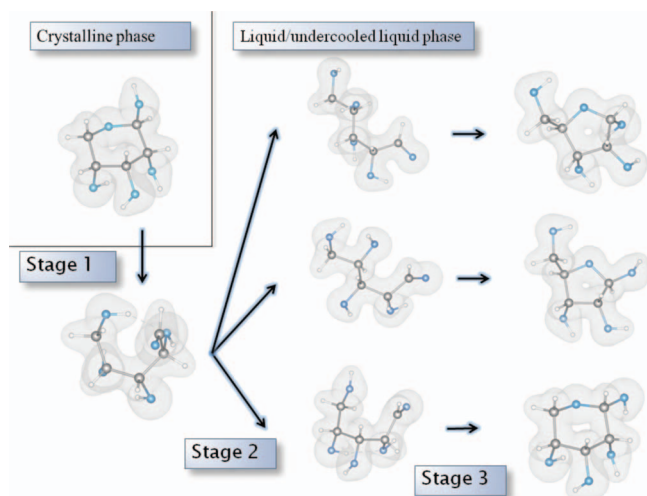


FIG. 4. Scheme of mutarotation after melting crystalline form (upper left corner). Every single process runs through open-chain stage.

tures and it is essential to know “direction” of mutarotation processes during forming equilibrium at room temperature. By knowing direction of the processes, one can predict which form has higher glass transition temperature. To know direction we have performed following analysis. Decrease of temperature (from melting point to room temperature) causes increase of most stable tautomer’s population, i.e., population of tautomer with lowest internal energy. By comparison of energy of isolated molecules, it may be concluded that pyranosidic form is usually more stable than furanosidic one. Unfortunately the problem is more complicated as population ratio is highly sensitive to the intermolecular interactions. For example, in DMSO (dimethyl sulfoxide) solvent, the most stable is furanosidic form of D-fructose, whereas in water environment pyranosidic tautomer is more preferable. Composition of tautomers in anhydrous D-fructose and

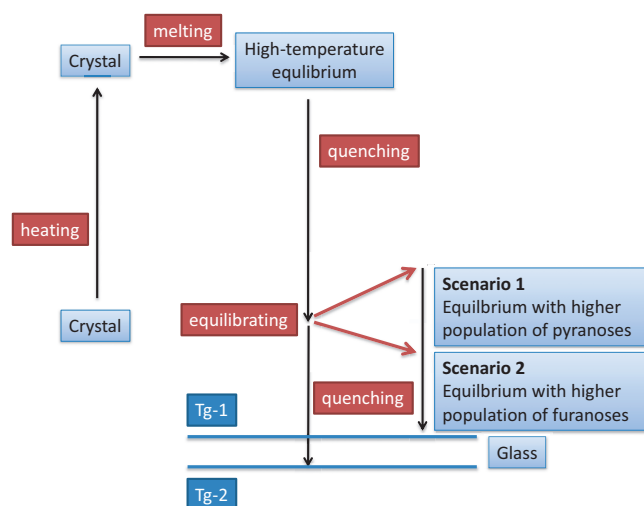


FIG. 5. Diagram represents formation of carbohydrate glass. After heating and melting crystalline sample tautomeric equilibrium is formed. When the sample is quenched to the glass, vitrification occurs at temperature labeled as  $T_{g-2}$ . If the sample is equilibrated in the vicinity of glass transition area (above  $T_g$ ) tautomeric ratios change due to the mutarotation process. This new equilibrium with higher population of furanoses or pyranoses has higher glass transition temperature, labeled as  $T_{g-1}$ .

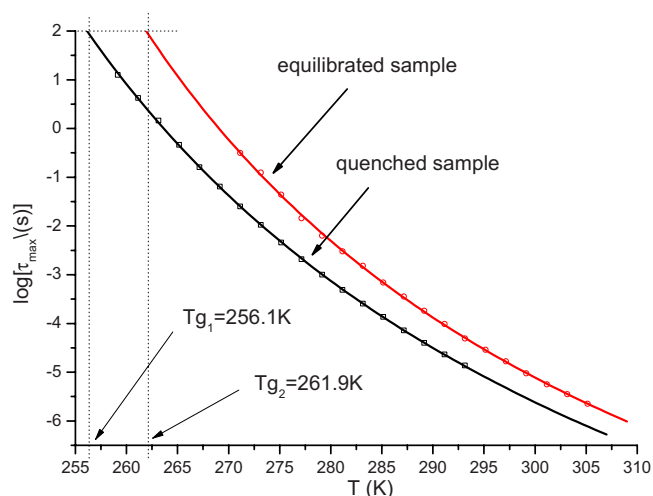


FIG. 6. Diagram represents dependencies of relaxation time logarithm versus temperature for quenched and equilibrated samples. Data were fitted to the Vogel–Fulcher–Tamman equation. One can note that sample equilibrated at room temperature has higher glass transition temperature

D-ribose is unknown, therefore, for every carbohydrate there are two possible scenarios of mutarotation after quenching melted sample to desired temperature. In the first scenario, pyranosidic tautomer is the most stable one and dielectric spectroscopy monitor mainly furanose to pyranose transformations. In the second scenario, furanoses are more stable in supercooled liquid state and dielectric spectroscopy monitor opposite conversions (pyranoses to furanoses).

Analysis of dipole moments of D-ribose as well as D-fructose indicates that first scenario is more probable for both of the sugars. In Table II one can find that pyranosidic forms of D-fructose have enormous dipole moment, while pyranosidic forms of D-ribose have rather low dipole moment. This can be easily connected with the behavior of static permittivity. Formation of pyranoses in D-fructose is manifested by increase of static permittivity in time and in D-ribose by decrease of static permittivity in time.

Very interesting aspect is the impact of mutarotation on local secondary mode observed in the glassy state. This mode is known as  $\gamma$ -process. Microscopic origin of this process has not been identified yet, however, one can expect that it arise from internal motions of molecule. One of them is change of the conformation of the ring. In case of pyranosidic ring, this is the chair to boat or chair to chair conversion. The second possibility is reorientation of exocyclic hydroxymethyl group  $-\text{CH}_2\text{OH}$ . Mutarotation has very strong

TABLE II. Dipole moments of particular tautomers of D-ribose and D-fructose. Dipole moments of D-ribose are calculated as weighted average from dipole moments of five most stable conformers, whereas dipole moments of d-fructose are presented for the one most stable conformer.

D-ribose		D-fructose	
Tautomer	Dipole moment (D)	Tautomer	Dipole moment (D)
$\beta$ -D-pyranose	2.15	$\beta$ -D-pyranose	3.54
$\beta$ -D-furanose	2.56	$\beta$ -D-furanose	0.66
$\alpha$ -D-furanose	3.21	$\alpha$ -D-furanose	2.94

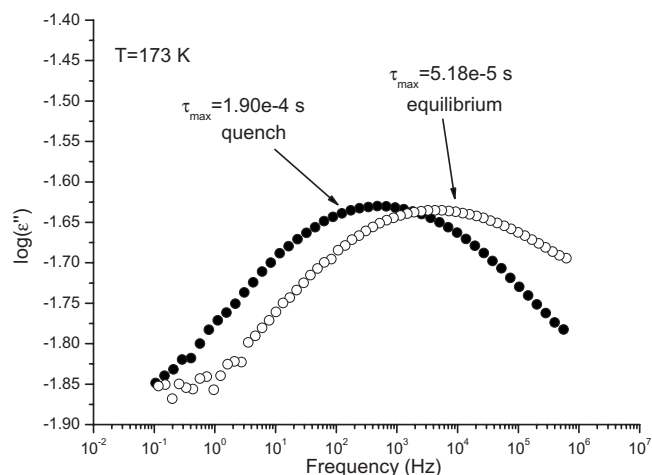


FIG. 7. Comparison of  $\gamma$ -process observed in the quenched melt and in the quenched equilibrium to the measurement temperature

impact on this motion. In D-fructose, amplitude of the  $\gamma$ -process increased about 50% during mutarotation,<sup>13</sup> whereas the relaxation time did not change at all. On the other hand, the effect is different in D-ribose. Dielectric strength is almost the same, while the relaxation time is shifted about 1 decade (at 193 K) toward higher frequencies. One can observe the change in dielectric spectra in Fig. 7. Moreover energy of activation diminished from 38 to 33 kJ/mol. See Fig. 8 for details. The discussion about origin of  $\gamma$ -relaxation will be discussed in separate paper which is in preparation.

#### IV. CONCLUSIONS

In summary, we performed measurements of kinetics of mutarotation of supercooled, anhydrous D-ribose in the temperature range 393–405 K. We have estimated two energies of activation for this process for D-ribose. First energy of activation is obtained from the analysis of relaxation times of  $\alpha$ -relaxation. Second energy is obtained from the analysis of static permittivity monitored during this phenomenon. We have also shown that high pressure (400 MPa) slows down

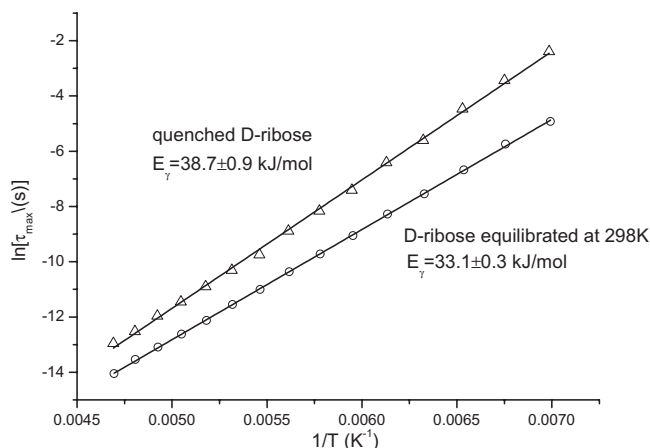


FIG. 8. Activation energies of  $\gamma$ -process after quenching and equilibrating sample

the mutarotation of anhydrous D-ribose by 20%. We have tried to find the direction of this process in the quenched melt. We have assumed that during the melting process, tautomeric equilibrium is achieved very quickly. After quenching the sample, equilibrium is shifted towards higher population of pyranoses in D-ribose as well as D-fructose, thus dielectric spectroscopy monitor furanose to pyranose transformations. It was determined by comparative studies of tautomers' dipole moments and static permittivity behavior. We have found that not only glass transition temperature but also relaxation time of  $\gamma$ -process is sensitive to the changes of pyranose/furanose ratio. Behavior of  $\gamma$ -relaxation during mutarotation of D-ribose has been revealed.

#### ACKNOWLEDGMENTS

The authors (P.W., K.K., M.D., S.H., and M.P.) are deeply thankful for the financial support of their research within the framework of the project entitled From Study of Molecular Dynamics in Amorphous Medicines at Ambient and Elevated Pressure to Novel Applications in Pharmacy, which is operated within the Foundation for Polish Science Team Programme cofinanced by the EU European Regional Development Fund. Moreover, P.W. would like to thank Foundation for Polish Science for awarding grants within the framework of the START Programme (2010).

- <sup>1</sup>K. N. Kirschner and R. J. Woods, *Proc. Natl. Acad. Sci. U.S.A.* **98**, 10541 (2001).
- <sup>2</sup>T. V. Chalikian, *J. Phys. Chem. B* **102**, 6921 (1998).
- <sup>3</sup>V. Molinero and W. A. Goddard, *Phys. Rev. Lett.* **95**, 045701 (2005).
- <sup>4</sup>H. Weingärtner, A. Knocks, S. Boresch, P. Hocht, and O. Steinhauser, *J. Chem. Phys.* **115**, 1463 (2001).
- <sup>5</sup>V. H. Tran and J. W. Brady, *Biopolymers* **29**, 961 (1990).
- <sup>6</sup>P. Włodarczyk, K. Kaminski, K. Adrjanowicz, Z. Wojnarowska, B. Czarnota, M. Paluch, J. Ziolo, and J. Pilch, *J. Chem. Phys.* **131**, 125103 (2009).
- <sup>7</sup>J. N. Reitter, R. E. Means, and R. C. Desrosiers, *Nat. Med.* **4**, 679 (1998).
- <sup>8</sup>K. Kaminski, E. Kaminska, P. Włodarczyk, S. Pawlus, D. Kimla, A. Kasprzycka, M. Paluch, J. Ziolo, W. Szeja, and K. L. Ngai, *J. Phys. Chem. B* **112**, 12816 (2008).
- <sup>9</sup>K. Kaminski, E. Kaminska, K. L. Ngai, M. Paluch, P. Włodarczyk, A. Kasprzycka, and W. Szeja, *J. Phys. Chem. B* **113**, 10088 (2009).
- <sup>10</sup>N. Dujardin, J. F. Willart, E. Dudognon, A. Hedoux, Y. Guinet, L. Paccou, B. Chazallon, and M. Descamps, *Solid State Commun.* **148**, 78 (2008).
- <sup>11</sup>*The Organic Chemistry of Sugars*, edited by D. E. Levy and P. Fugedi (CRC, Boca Raton, 2006).
- <sup>12</sup>J. F. Robyt, *Essentials of Carbohydrate Chemistry* (Springer-Verlag, New York, 1998).
- <sup>13</sup>P. Włodarczyk, K. Kaminski, M. Paluch, and J. Ziolo, *J. Phys. Chem. B* **113**, 4379 (2009).
- <sup>14</sup>P. Włodarczyk, K. Kaminski, M. Dulski, S. Haracz, M. Paluch, and J. Ziolo, *J. Non-Cryst. Solids* **356**, 738 (2010).
- <sup>15</sup>R. Lefort, V. Caron, J.-F. Willart, and M. Descamps, *Solid State Commun.* **140**, 329 (2006).
- <sup>16</sup>N. L. Barch, J. M. Grossel, P. Looten, and M. Mathlouthi, *Food Chem.* **74**, 119 (2001).
- <sup>17</sup>A. M. Silva, E. C. da Silva, and C. O. da Silva, *Carbohydr. Res.* **341**, 1029 (2006).
- <sup>18</sup>R. Behrends and U. Kaatz, *Biophys. Chem.* **111**, 89 (2004).
- <sup>19</sup>F. Neese, Orca—An *Ab Initio*, Density Functional and Semiempirical Program Package, Version 2.5, University of Bonn, 2006.
- <sup>20</sup>F. V. Sander, *J. Biol. Chem.* **148**, 311 (1943).
- <sup>21</sup>B. Andersen and F. Gronlund, *Acta Chem. Scand., Ser. A* **33a**, 275 (1979).